

Axial Ratio Bandwidth Enhancement of 60-GHz Substrate Integrated Waveguide-Fed Circularly Polarized LTCC Antenna Array

Yue Li, *Student Member, IEEE*, Zhi Ning Chen, *Fellow, IEEE*, Xianming Qing, *Member, IEEE*, Zhijun Zhang, *Senior Member, IEEE*, Junfeng Xu, *Member, IEEE*, and Zhenghe Feng, *Fellow, IEEE*

Abstract—A substrate integrated waveguide (SIW)-fed circularly polarized (CP) antenna array with a broad bandwidth of axial ratio (AR) is presented for 60-GHz wireless personal area networks (WPAN) applications. The widened AR bandwidth of an antenna element is achieved by positioning a slot-coupled rotated strip above a slot cut onto the broadwall of an SIW. A 4×4 antenna array is designed and fabricated using low temperature cofired ceramic (LTCC) technology. A metal-topped via fence is introduced around the strip to reduce the mutual coupling between the elements of the array. The measured results show that the AR bandwidth is more than 7 GHz. A stable boresight gain is greater than 12.5 dBic across the desired bandwidth of 57–64 GHz.

Index Terms—Antenna array, axial ratio, circular polarization, low temperature cofired ceramic, substrate integrated waveguide.

I. INTRODUCTION

WITH THE progress in high data rate wireless technologies, wireless personal area networks (WPAN) with an available spectrum of 57–64 GHz have been proposed for short-range communication applications [1]. Due to high operating frequencies and wide operating bandwidth, the design of antennas at 60-GHz bands becomes challenging [2], [3]. Low temperature cofired ceramic (LTCC) technology is an excellent candidate for the millimeter wave (mmW) antenna design because of its merits of multilayer configuration, flexible metalization, and low fabrication tolerance [3]–[6]. Compared with conventional multilayer print circuit board (PCB) technology, the LTCC technology is easier in the realization of blind vias and across-layer connection by vias.

Manuscript received November 10, 2011; revised January 09, 2012; accepted May 14, 2012. Date of publication July 10, 2012; date of current version October 02, 2012. This work was supported by the National Basic Research Program of China under Contract 2009CB320205, by the National High Technology Research and Development Program of China (863 Program) under Contract 2011AA010202, the National Science and Technology Major Project of the Ministry of Science and Technology of China 2010ZX03007-001-01, and in part by Qualcomm Inc.

Y. Li, Z. Zhang, and Z. Feng are with State Key Laboratory on Microwave and Digital Communications, Tsinghua National Laboratory for Information Science and Technology, Department of Electronic Engineering, Tsinghua University, Beijing 100084, China (e-mail: hardy_723@163.com; zjzhang5@gmail.com; fzh-dee@mail.tsinghua.edu.cn).

Z. N. Chen, X. Qing, and J. F. Xu are with the Institute for Information Research, Singapore, Agency of Science, Technology, and Research, Singapore 138642, Singapore (e-mail: chenzn@i2r.a-star.edu.sg; qingxm@i2r.a-star.edu.sg; jxu@i2r.a-star.edu.sg).

Color versions of one or more of the figures in this paper are available online at <http://ieeexplore.ieee.org>.

Digital Object Identifier 10.1109/TAP.2012.2207343

To compensate for the high path loss at mmW bands, an antenna array with high gain is more preferable for mmW systems. However, the gain enhancement of the antenna array is limited by the loss caused by its feeding network, such as a microstrip-line feeding network. Therefore, substrate integrated waveguide feeding network is widely used at the mmW bands because of its low transmission loss [7].

Furthermore, the circularly polarized (CP) antenna arrays have been used to improve the quality of the high-speed wireless links at the 60-GHz bands [8], [9]. However, the operating bandwidth of 7 GHz for both impedance matching and axial ratio (AR) is really a challenge for antenna design. Several methods were proposed to improve the AR bandwidth of an antenna array [10]–[13]. For example, a 4×2 circularly polarized slot array loaded by ellipse strip was proposed [10], achieving a bandwidth of 34.6% for the AR lower than 3.3 dB at 60 GHz with the gain greater than 8 dBi. A 2×2 circularly polarized cavity-backed aperture antenna array was reported with the AR bandwidth of 50% at 10 GHz with the gain greater than 6 dBic [11]. It should be noted that the designs presented in [10]–[13], the sequentially rotated feed technique was used to achieve the AR bandwidth. Such feeding structures are easily configured by a microstrip-line structure which may cause high loss at mmW bands. The CP array designs achieved the 3-dB AR bandwidth of 4% at the 60-GHz bands [8], [9]. Therefore, the combined design considerations of the AR bandwidth, gain, and feeding structure complexity become the unique design challenge at the mmW bands.

In [14]–[17], a CP antenna was designed using a waveguide-fed structure, and also for the array applications at 12 GHz. The CP antenna consists of a slot-coupled rotated dipole above the feeding slot cut onto the broadwall of a waveguide. Such a dipole-slot antenna has the merits of simple feeding structure and geometry, suitable for SIW-fed antenna array design on LTCC. However, such an antenna element and array suffer narrow AR bandwidth, typically of 4%.

In this paper, a slot-coupled rotated strip with a metal-topped via fence is proposed as an element to widen the AR bandwidth of an antenna array operating at the 60-GHz bands. A 4×4 SIW-fed CP antenna array is fabricated using LTCC technology and tested.

II. ANTENNA ELEMENT DESIGN

Fig. 1 shows the proposed antenna element. It is composed of a 10-layer LTCC substrate of Ferro A6-M with $\epsilon_r = 5.9 \pm 0.2$,

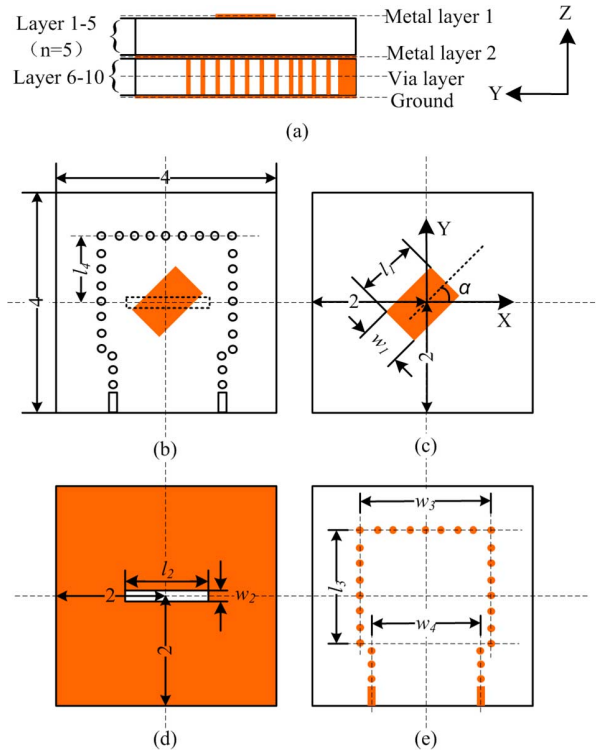


Fig. 1. Geometry and dimensions of the proposed antenna element on LTCC (unit: mm): (a) side view; (b) top view; (c) metal layer 1; (d) metal layer 2; (e) middle layer.

TABLE I
DETAILED DIMENSIONS OF THE ELEMENT (UNIT: MM)

l_1	w_1	α	l_2	w_2	l_3	w_3	l_4	w_4
0.92	0.44	45°	1.1	0.2	1.75	2	1.25	1.8

$\tan \delta = 0.002$ at 60 GHz. The thickness of the substrate layer is $b = 0.095$ mm and the metal layer $t = 0.015$ mm. The conductor used (in dark color) for the metallization and vias is Au with the conductivity of 4.56×10^7 S/m. The antenna element comprises three parts: a rectangular strip rotated by an angle of α from x -axis, a feeding slot cut onto the broadwall of the SIW, and a cavity at the end of the SIW for impedance matching. The SIW feeding structure is formed in Layers 6–10 and the strip is positioned five layers above the feeding slot. The diameter and the pitch of the vias in the SIW are 0.1 and 0.25 mm, respectively.

The detailed optimized parameters are tabulated in Table I. The optimization is conducted using the software package of CST Microwave Studio that is based on a finite integration method. Figs. 2 and 3 show the simulated reflection coefficient, AR bandwidth, and gain of the antenna element. The bandwidths of the -10 dB reflection coefficient and the 3 dB AR cover the 60-GHz WPAN band of 57–64 GHz. Within the operating bandwidth, the gain is greater than 4.59 dBi.

The dipole-slot antenna can be used to generate CP radiation as shown in [14]–[17]. In order to widen the AR bandwidth of dipole-slot structure, a rectangular patch is used to replace the thin dipole as shown in Fig. 1. The patch element introduces additional CP radiation because the additional one-wavelength mode appears along the edge of the patch element where the current is excited.

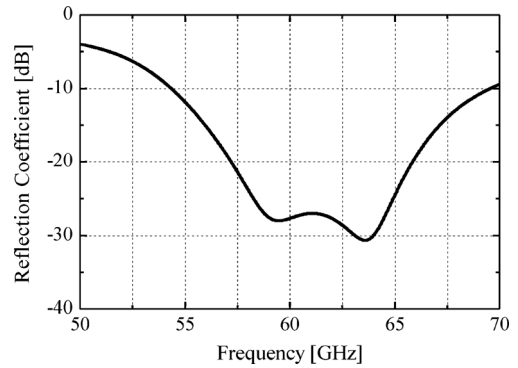


Fig. 2. Simulated reflection coefficient of the antenna element.

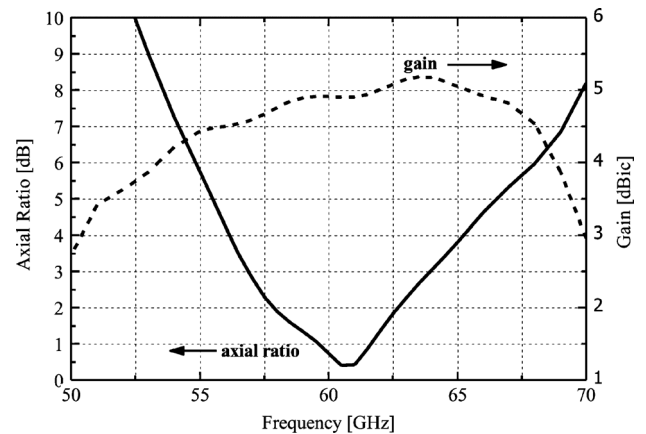


Fig. 3. Simulated AR and gain of the antenna element.

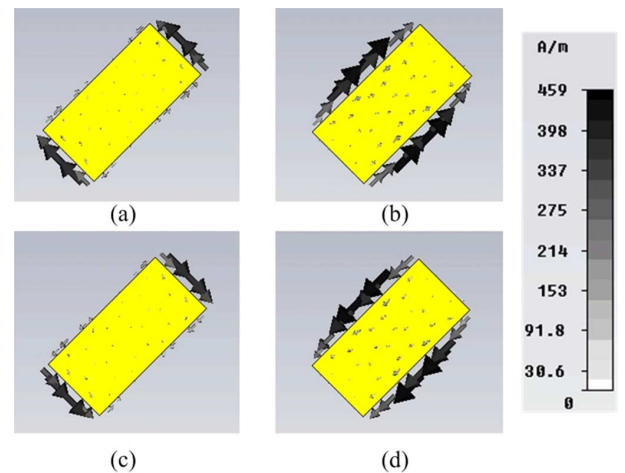


Fig. 4. Current distribution on a rotated patch at 60 GHz with different phase: (a) 0°; (b) 90°; (c) 180°; (d) 270°.

As shown in Fig. 4, two one-wavelength modes are at the edges of patch. At the phase of 0°, 90°, 180°, and 270°, the current appearing periodically along the broad or narrow edges of the patch flows in a rotated direction, which generates a left-hand CP radiation. Such additional CP radiation broadens the overall AR bandwidth up to 7.16 GHz (56.91–64.07 GHz) as shown in Fig. 3.

The AR bandwidth is sensitive to slot and patch-related parameters, namely the thickness of the substrate layer (b), the rotated angle of the strip (α), as well as the dimensions of the

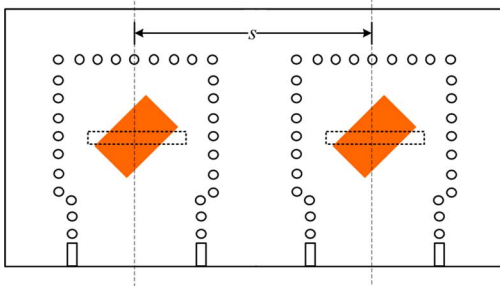
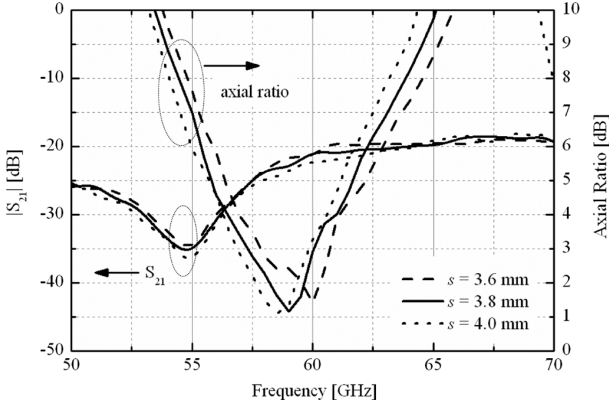


Fig. 5. Two-element array.

Fig. 6. Simulated $|S_{21}|$ and AR with different s .

strip (l_1 and w_1). The spacing between the strip and slot determines the phase difference of orthogonal modes. The rotated angle (α) of the strip is tuned to achieve the equal amplitudes for the orthogonal modes. The center frequency of AR bandwidth shifts down as increasing α . The dimensions of the strip (l_1 and w_1) affect the center frequency of the AR bandwidth. The dimensions of the feeding slot (l_2 and w_2) have less effect to AR bandwidth. However, the feeding slot is important for energy coupling to the rotated strip. It is also found that the parameters l_4 , l_3 , and w_3 hardly affect the CP performance but impedance matching. The cavity at the end of the SIW acts as an impedance transformer between the feeding slot and the SIW.

III. ANTENNA ARRAY DESIGN

The mutual coupling between the two adjacent elements of the array is examined. Fig. 5 shows the array configuration with two proposed elements separated at a center distance s . The $|S_{21}|$ and AR response with different s are simulated as shown in Fig. 6. Clearly, the AR bandwidth reduces dramatically from 11.7% in Fig. 3 to 4.2% in Fig. 6 because of the interelement mutual coupling.

A. Mutual Coupling Reduction

The mutual coupling is mainly caused by the surface wave between the elements. The surface wave propagates along the metal Layer 2, where the feeding slot is positioned. Due to the surface wave, the phase difference between two orthogonal modes in single element has been changed. To maintain the AR bandwidth in the array environment, the mutual coupling must be reduced. In [18], a metal-topped quarter-wavelength type choke structure is designed to suppress the surface waves.

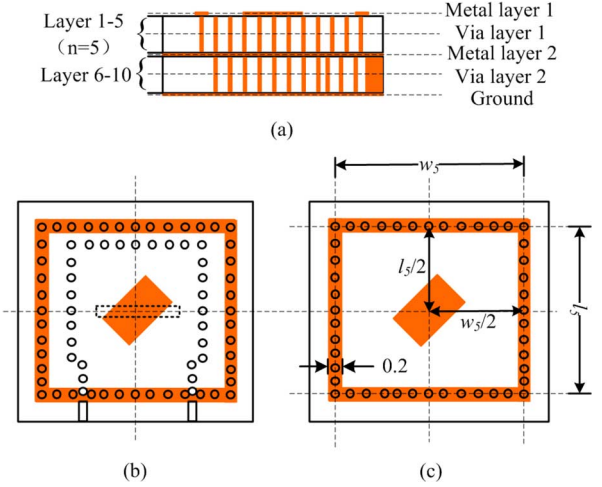
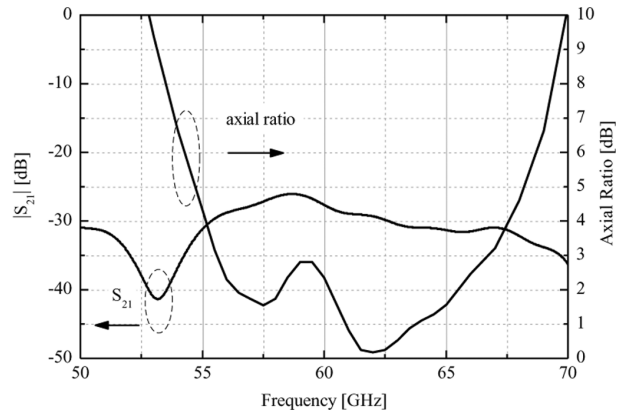


Fig. 7. Geometry of the proposed element with metal-topped via fence (Unit: mm). (a) side view; (b) top view; (c) metal layer 1.

Fig. 8. Simulated $|S_{21}|$ and AR with $s = 3.8$ mm.

To maintain the magnetic boundary condition to the radiating aperture, the choke is positioned at a distance of approximately a half wavelength from the radiating element. However, in the array design, the distance between two adjacent elements is restricted by other radiation performance, such as sidelobe level and so on. Therefore, we propose a metal-topped via fence around the element with a small distance to block the surface waves as shown in Fig. 7. The uniform width of the metal top is 0.2 mm. The distance l_5 and w_5 are optimized for both the AR bandwidth and impedance matching with $l_5 = w_5 = 3$ mm ($0.6\lambda_0$ at 60 GHz). Between two elements, two rows of via-fence are positioned to block the surface waves.

The effect of the via-fence on the AR of the two-element array and the interelement mutual coupling is shown in Fig. 8. The AR bandwidth is much wider than that without the via-fence as shown in Fig. 6, and is even wider than the single element. The isolation between the two adjacent elements is also improved more than 25 dB using the metal-topped via-fence.

The single element with a metal-topped via-fence has also been simulated. Figs. 9 and 10 show the simulated reflection coefficient, AR bandwidth, and gain. The via-fence operates as a cavity load, which is helpful for impedance bandwidth improvement [3]. The cavity loading also provides additional freedom

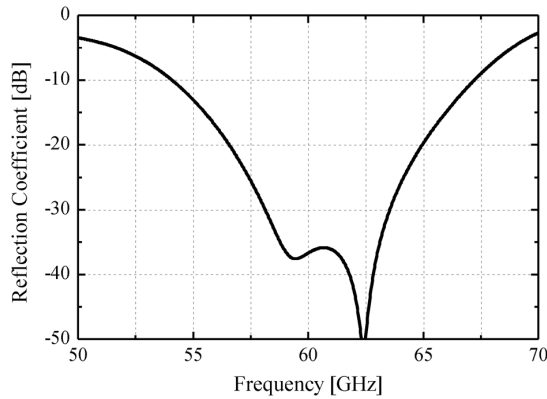


Fig. 9. Simulated reflection coefficient of the single antenna element with metal-topped via-fence.

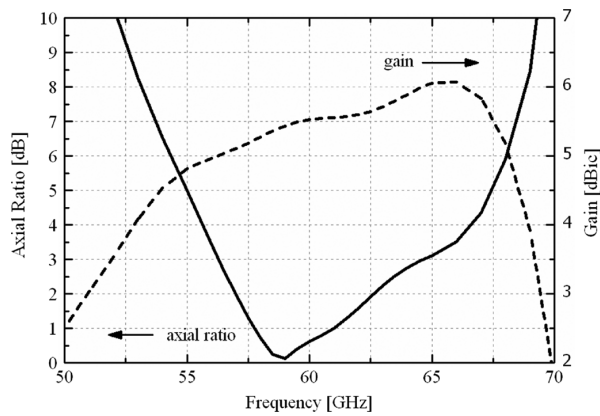


Fig. 10. Simulated AR and gain of the single antenna element with metal-topped via-fence.

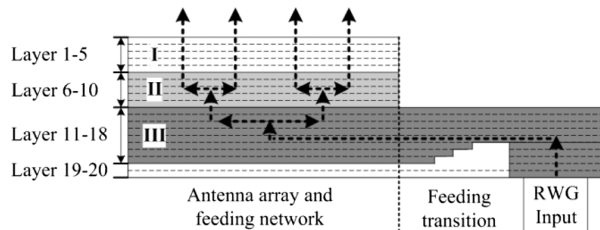


Fig. 11. Side view of the 4×4 -element array with feed transition.

in AR optimization by tuning l_5 and w_5 . The reflection of surface wave can be utilized to tune the amplitudes in orthogonal directions. Due to cavity effect, the gain of single element is also increased as shown in Fig. 10.

B. Antenna Array With Feeding Structure

Fig. 11 shows the 4×4 -element antenna array with the feeding network on the left hand side and the stepped feeding transition for measurement on the right hand side. The feeding network and transition are modified from the feeding structure of [3]. A 20-layered LTCC substrate is used with the total thickness of 2.02 mm (20 substrate layers and 8 metal layers). The arrow with a dashed line indicates the RF signal trace. The antenna array has three regions, which are shown in Figs. 12–14.

Region I includes five layers (Layers 1–5). The 16 elements are positioned with a distance of 3.8 mm ($0.76\lambda_0$ at 60 GHz)

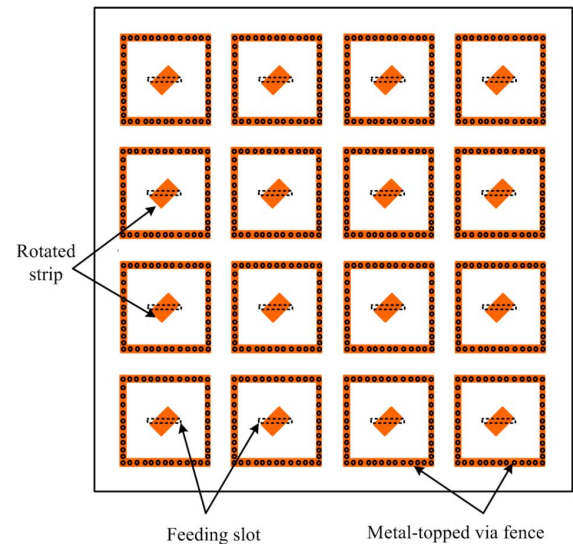


Fig. 12. Top view of Region I.

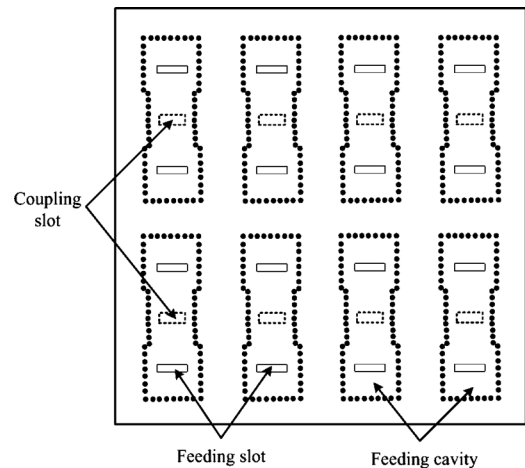


Fig. 13. Top view of region II.

between two adjacent elements in both horizontal and vertical directions. The rotated strip and metal top of the via-fence are printed on the top layer (Layer 1), and the via-fence is formed from Layer 1 to 5. As shown in Fig. 13, Region II also includes five layers (Layers 6–10). The 4×2 -element subarrays with feeding cavities and feeding slots (solid line) are arranged to feed the element. The feeding slots are etched onto the top of Layer 6, and the cavity is formed from Layer 6 to 10. Each subarray couples from Region III by a coupling slot (dashed line). The coupling slot is etched onto the top of Layer 11. The Region III includes 10 layers (Layers 11–20). As shown in Fig. 14, a 1-to-8 power divider is arranged from Layer 11 to 18 to couple the energy to the subarrays through the slots. The detailed dimensions of the power divider are illustrated in Fig. 15. Another part of Region III is the SIW-RWG transition with 10 layers (layer 11–20). The antenna array is fed through a WR-15 RWG. The stepped transition serves as an impedance transformer between the RWG and SIW in Layers 11–18 [3]. Fig. 16 shows the detailed dimensions of the transition. The optimized dimensions of the elements in the array are: $\alpha = 39^\circ$, $l_5 = w_5 = 2.8$ mm, and the other parameters are kept the same as the element design.

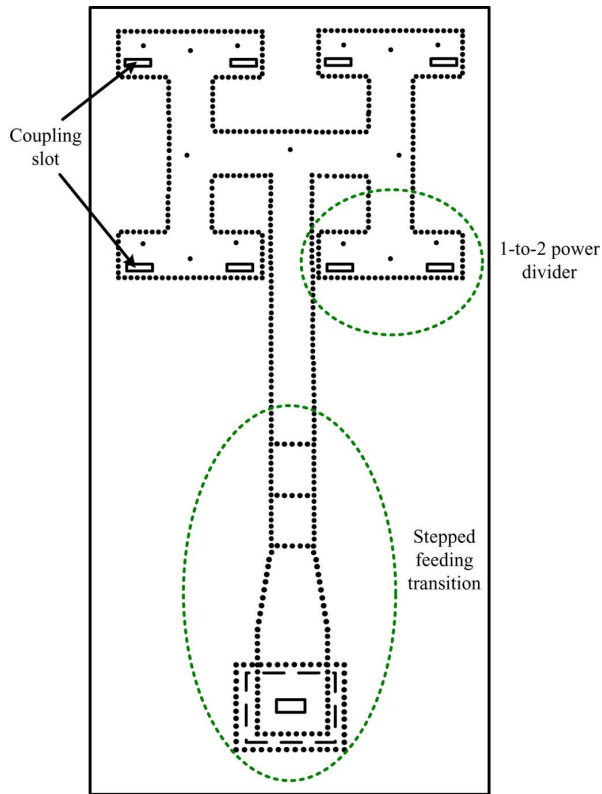


Fig. 14. Top view of Region III.

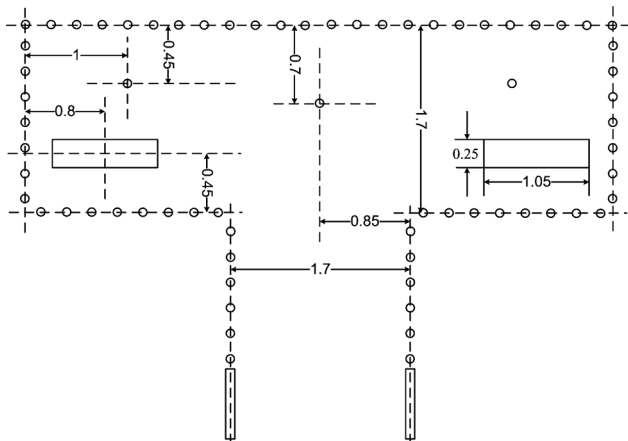


Fig. 15. Geometry and dimensions of the 1-to-2 power divider.

IV. EXPERIMENTAL RESULTS

The proposed 4×4 -element array with feeding transition was fabricated using LTCC as shown in Fig. 17(a). The overall size of the antenna area (white color) is $15.4 \times 15.4 \text{ mm}^2$. The holes in the feeding area are used for connecting and accurately positioning with the RWG flange. The antenna was measured using a self-built mmW antenna measurement system at Institute for Infocomm Research, Singapore, as shown in Fig. 17(b).

The measured results of the proposed antenna array are illustrated in Figs. 18 and 19, and compared with simulated results. The bandwidth of reflection coefficient better than -6 dB is from 56.65 GHz to 65.75 GHz . The measured 3 dB AR bandwidth ranges from 60.2 GHz , up to 67 GHz (due to the limitation of vector network analyzer). The measured AR bandwidth

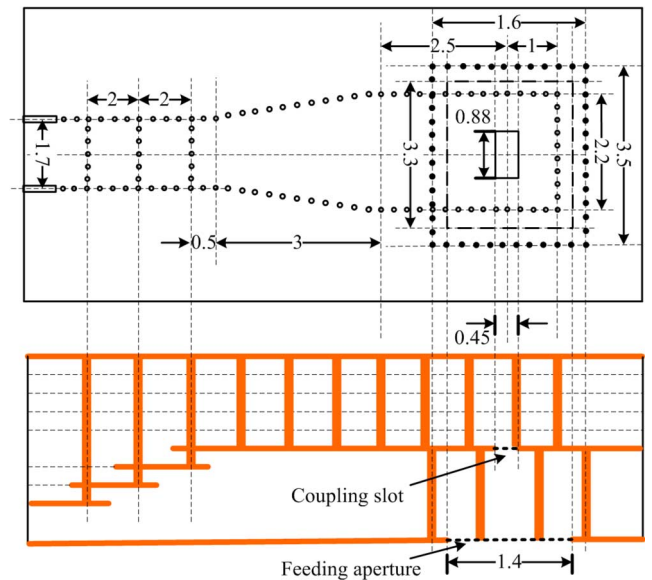


Fig. 16. Geometry and dimensions of the stepped feeding transition in Region III.

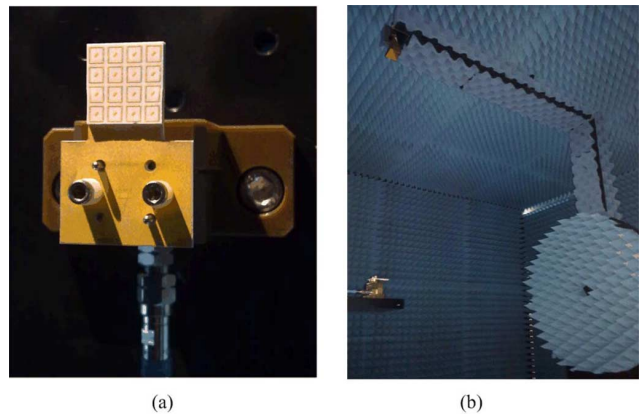


Fig. 17. Photograph of (a) array prototype and (b) measurement system.

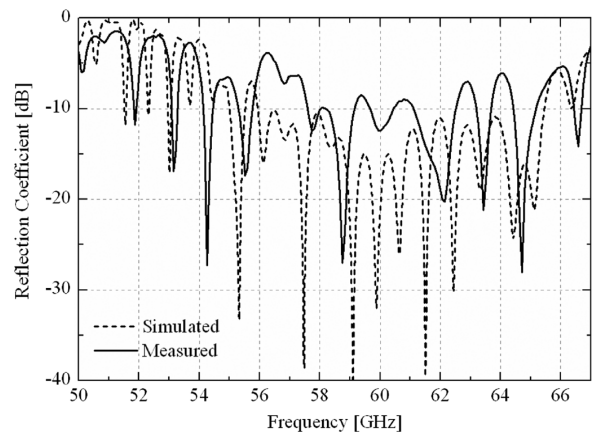


Fig. 18. Simulated and measured reflection coefficient of the antenna array.

of more than 7 GHz is as wide as the simulated while the band shifts to the higher end, which is mainly from the shrinking of LTCC fabrication.

The parametric study of the substrate layer thickness (b) is illustrated in Figs. 20 and 21. In Fig. 20, the decreasing b degrades the AR and shifts the resonant frequency upwards. And the

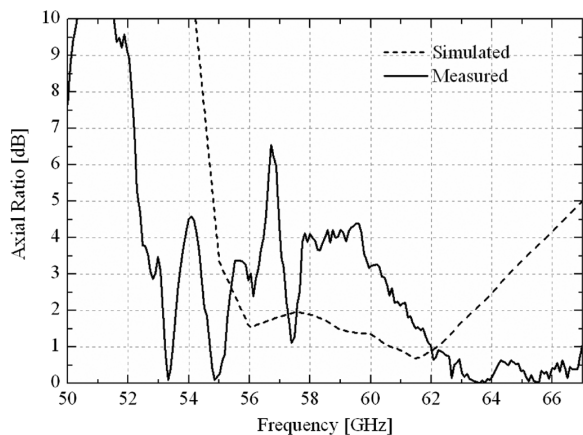


Fig. 19. Simulated and measured axial ratio of the antenna array.

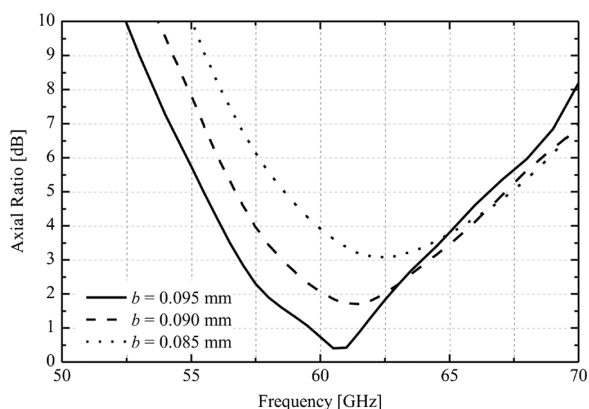


Fig. 20. Simulated AR of the antenna element with different b .

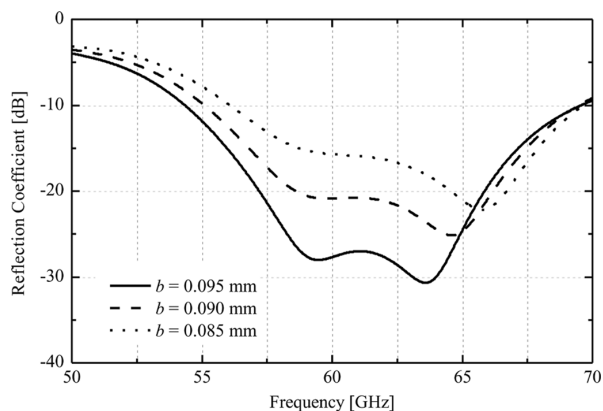


Fig. 21. Simulated reflection coefficient of the antenna element with different b .

impedance matching is also deteriorated as illustrated in Fig. 21. The thicknesses difference of the antenna prototype is observed as shown in Fig. 22. Compared with the designed thickness of 2.02 mm, the thickness of the antenna prototype is smaller and varies over the area of the antenna array. As discussed above, the reduction of the substrate thickness degrades the AR as well as the impedance matching bandwidth, and shifts the operating frequency upwards. The measurement validates the fact that the proposed method is capable of enhancing the AR bandwidth in array design with the SIW feeding structure in LTCC.

The normalized gain patterns of the proposed antenna array were measured and simulated in the xz -plane and yz -plane at

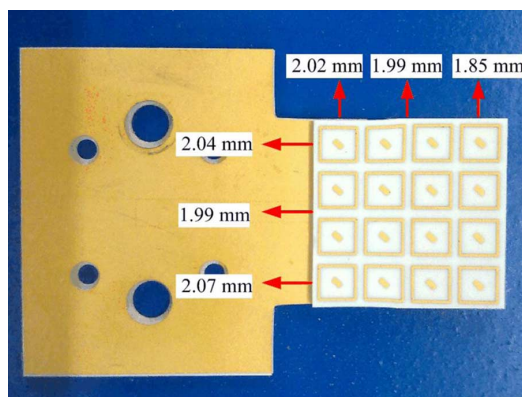
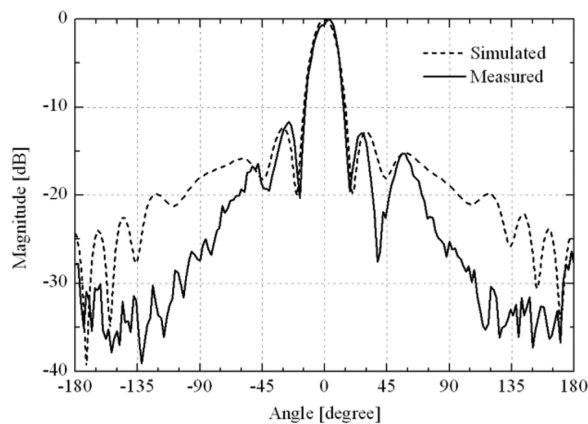
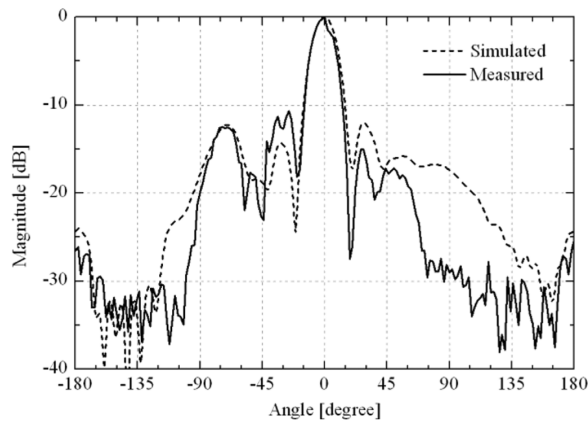


Fig. 22. The thicknesses of the antenna prototype at different positions.



(a)



(b)

Fig. 23. Simulated and measured radiation patterns of the antenna array at 60 GHz. (a) xz -plane. (b) yz -plane.

60 GHz. Usually, the gain as well as the radiation patterns of a CP antenna can be measured using the method of rotating a linear source [19]. Limited to the measurement set-up at 60 GHz bands, the gain with the horizontal and vertical polarizations instead of the gain aligned with the major and minor axes of the polarization ellipse are measured first and added together afterwards. The measurement shows good agreement with the simulation. In each plane, we measured the CP gain of the antenna at each angle and then normalized the results to the peak gain as shown in Fig. 23. The simulated and the measured sidelobe levels are lower than -10 dB.

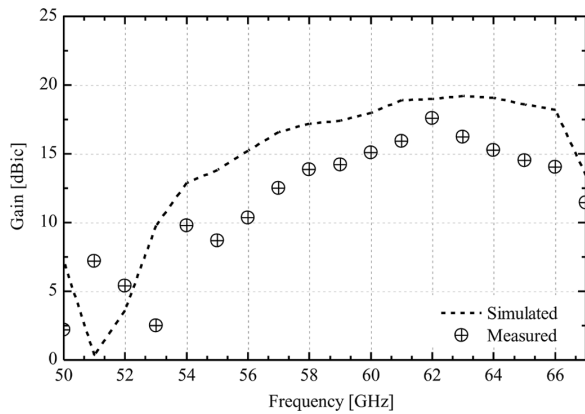


Fig. 24. Simulated and measured gains of the antenna array.

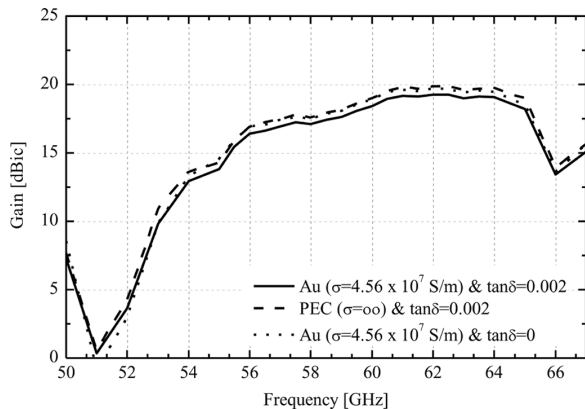


Fig. 25. Simulated gain of the antenna array with different substrates and metals.

Fig. 24 shows the measured gain of the proposed 4×4 antenna array. In the band of 57–64 GHz, the average gain is 15 dBic. Compared with the simulated results, an average gain drop of 2.5 dB comes from the deterioration of impedance matching due to the fabrication, also the deviation of the dielectric loss of the LTCC substrate and the conductivity of the metallization. Fig. 25 shows approximately 0.5 dB loss caused by the dielectric loss and metal conductivity.

V. CONCLUSION

In this paper, a 4×4 -element SIW-fed CP antenna array on LTCC has been proposed for 60-GHz applications. The AR bandwidth has been widened by adopting a rotated strip because of the additional CP radiation from the strip. In order to reduce the mutual coupling among elements in the array, a metal-topped via fence has been used to suppress the surface waves, also improve the AR bandwidth. A prototype of the proposed array has been fabricated and characterized in terms of impedance matching, AR bandwidth, radiation patterns, and gain. The measured results have shown that the 3 dB AR bandwidth covering 60.2–67 GHz has been achieved with the bore-sight gain greater than 12.5 dBic.

REFERENCES

[1] T. Zwick, D. Liu, and B. P. Gaucher, "Broadband planar superstrate antenna for integrated millimeterwave transceivers," *IEEE Trans. Antennas Propag.*, vol. 54, no. 10, pp. 2790–2796, Oct. 2006.

[2] D. Pozar, S. Targonski, and H. Syrigos, "Design of millimeter wave microstrip reflectarrays," *IEEE Trans. Antennas Propag.*, vol. 45, no. 2, pp. 287–296, Feb. 1997.

[3] J. Xu, Z. N. Chen, X. Qing, and W. Hong, "Bandwidth enhancement for a 60 GHz substrate integrated waveguide fed cavity array antenna on LTCC," *IEEE Trans. Antennas Propag.*, vol. 59, no. 3, pp. 826–832, Marc. 2011.

[4] M. Sun, Y. P. Zhang, K. M. Chua, L. L. Wai, D. Liu, and B. P. Gaucher, "Integration of Yagi antenna in LTCC package for differential 60-GHz radio," *IEEE Trans. Antennas Propag.*, vol. 56, no. 8, pp. 2780–2783, Aug. 2008.

[5] A. Lamminen, J. Säily, and A. Vimpri, "60-GHz patch antennas and arrays on LTCC with embedded-cavity substrates," *IEEE Trans. Antennas Propag.*, vol. 56, no. 9, pp. 2865–2874, Sep. 2008.

[6] T. Seki, N. Honma, K. Nishikawa, and K. Tsunekawa, "60-GHz multilayer parasitic microstrip array antenna on LTCC substrate for system-on-package," *IEEE Microw. Wireless Compon. Lett.*, vol. 15, no. 5, pp. 339–341, May 2005.

[7] H. Yoshida, Y. Sakamoto, U. Klein, and T. Endo, "Improvements in the millimeter-wave subsystem for Josephson junction array voltage standard systems," *IEEE Trans. Microw. Theory Techn.*, vol. 41, no. 12, pp. 2353–2358, Dec. 1993.

[8] R. Zhou, D. Liu, and H. Xin, "Design of circularly polarized antenna for 60 GHz wireless communications," in *Proc. 3rd Eur. Conf. Antennas Propag.*, 2009, pp. 3787–3789.

[9] S. Pinel, I. K. Kim, K. Yang, and J. Laskar, "60 GHz linearly and circularly polarized antenna arrays on liquid crystal polymer substrate," in *Proc. 36th Eur. Microw. Conf.*, 2006, pp. 858–861.

[10] A. R. Weily and Y. J. Guo, "Circularly polarized ellipse-loaded circular slot array for millimeter-wave WPAN applications," *IEEE Trans. Antennas Propag.*, vol. 57, no. 10, pp. 3680–3684, Oct. 2009.

[11] K.-F. Hung and Y.-C. Lin, "Novel broadband circularly polarized cavity-backed aperture antenna with traveling wave excitation," *IEEE Trans. Antennas Propag.*, vol. 58, no. 1, pp. 35–42, Jan. 2010.

[12] M. Shahabadi, D. Busuico, A. Borji, and S. Safavi-Naeini, "Low-cost, high-efficiency quasi-planar array of waveguide-fed circularly polarized microstrip antennas," *IEEE Trans. Antennas Propag.*, vol. 53, no. 6, pp. 2036–2043, Jun. 2005.

[13] J. Huang, "A Ka-band circularly polarized high-gain microstrip array antenna," *IEEE Trans. Antennas Propag.*, vol. 43, no. 1, pp. 113–116, Jan. 1995.

[14] K. Itoh and T. Adachi, "Novel circularly polarized antennas combining a slot with parasitic dipoles," in *Proc. IEEE Antennas Propag. Soc. Int. Symp.*, 1980, pp. 52–55.

[15] J. Hirokawa, T. Nanbu, M. Ando, and N. Goto, "Circularly-polarized waveguide array with slots and dipoles," in *Proc. IEEE Antennas Propag. Soc. Int. Symp.*, 1991, pp. 1338–1341.

[16] K.-S. Min, J. Hirokawa, K. Sakurai, and M. Ando, "Phase control of circularly polarized waves from a parasitic dipole mounted above a slot," in *Proc. IEEE Antennas Propag. Soc. Int. Symp.*, 1997, pp. 1348–1351.

[17] K.-S. Min, J. Hirokawa, K. Sakurai, M. Ando, and N. Goto, "Single-layer dipole array for linear-to-circular polarization conversion of slotted waveguide array," in *IEE Proc. Microw., Antennas Propag.*, 1996, vol. 143, pp. 211–216.

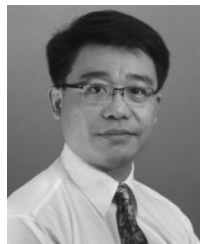
[18] R. Li, G. DeJean, M. M. Tentzeris, J. Papapolymerou, and J. Laskar, "Radiation-pattern improvement of patch antennas on a large-size substrate using a compact soft-surface structure and its realization on LTCC multilayer technology," *IEEE Trans. Antennas Propag.*, vol. 53, no. 1, pp. 200–208, Jan. 2005.

[19] B.-Y. Toh, R. Cahill, and V. F. Fusco, "Understanding and measuring circular polarization," *IEEE Trans. Educ.*, vol. 46, no. 3, pp. 313–318, Aug. 2003.



Yue Li (S'11) was born in Shenyang, Liaoning Province, China, in 1984. He received the B.S. degree in telecommunication engineering from the Zhejiang University, Zhejiang, China, in 2007. He is currently working toward Ph.D. degree in electrical engineering from Tsinghua University, Beijing, China.

His current research interests include antenna design and theory, particularly in reconfigurable antennas, electrically small antennas, and antenna in package.



Zhi Ning Chen (F'08) received the B.Eng., M.Eng., and Ph.D. degrees, all in electrical engineering, from the Institute of Communications Engineering (ICE), China, in 1985, 1988, 1993, respectively, and a second Ph.D. degree from University of Tsukuba, Japan, in 2003

From 1988 to 1995, he worked at ICE as a Lecturer and later as an Associate Professor. He also worked at Southeast University, China, as a Postdoctoral Fellow and later as an Associate Professor. During 1995–1997, he joined the City University of Hong

Kong as a Research Assistant and later, as a Research Fellow. In 1997, he was awarded the Japan Society for the Promotion of Science (JSPS) Fellowship to conduct his research at the University of Tsukuba. In 2001 and 2004, he visited the University of Tsukuba under a JSPS Fellowship Program (senior level). In 2004, he worked at IBM T. J. Watson Research Center as an Academic Visitor. During 1999–2012, he worked with the Institute for Infocomm Research (I2R) (formerly known as Centre for Wireless Communications and Institute for Communications Research) as Member of Technical Staff (MTS), Senior MTS, Principal MTS, Senior Scientist, Lead Scientist, and Principal Scientist as well as Head for RF & Optical Department. Since 2012, he has been with the Department of Electrical and Computer Engineering, National University of Singapore as a Professor and is concurrently holding a joint appointment in I2R, as well as Visiting/Adjunct/Guest Professor positions at Southeast University, Nanjing University, Shanghai Jiaotong University, Tsinghua University, Tongji University, University of Science and Technology, China, Dalian Maritime University, and City University of Hong Kong. His current research interests include engineering electromagnetics, antennas for microwaves, mmW, submmW, and THz systems. He has published 380 technical papers and authored/edited the books entitled *Broadband Planar Antennas*, *UWB Wireless Communication*, *Antennas for Portable Devices*, and *Antennas for Base Stations in Wireless Communications*. He also contributed to the books *UWB Antennas and Propagation for Communications, Radar, and Imaging*, *Antenna Engineering Handbook* as well as *Microstrip and Printed Antennas*. He holds 27 granted and filed patents with 31 licensed deals with industry.

Dr. Chen is the recipient of International Symposium on Antennas and Propagation Best Paper Award 2010, the CST University Publication Award 2008, IEEE AP-S Honorable Mention Student Paper Contest 2008, IES Prestigious Engineering Achievement Award 2006, I2R Quarterly Best Paper Award 2004, and IEEE iWAT 2005 Best Poster Award. He currently serves as an Associate Editor for the IEEE TRANSACTIONS ANTENNAS AND PROPAGATION and served as a Distinguished Lecturer for the IEEE Antennas and Propagation Society. He has been the Founding General Chairs of International Workshop on Antenna Technology (iWAT), International Symposium on InfoComm and Media Technology in Biomedical and Healthcare Applications (IS 3T-in-3A), International Microwave Forum (IMWF) as well as Asia-Pacific Conference on Antennas and Propagation (APCAP).



Xianming Qing (M'02) received the B.Eng. degree from University of Electronic Science and Technology of China (UESTC), Chengdu, in 1985, and the Ph.D. degree from Chiba University, Chiba, Japan, in 2010.

During 1987–1996, he was with UESTC for teaching and research and appointed as a Lecturer in 1990 and an Associate Professor in 1995. He joined National University of Singapore (NUS) in 1997 as a Research Scientist. Since 1998, he has been with the Institute for Infocomm Research (I2R, formerly known as CWC and ICR), Singapore. He is currently holding the position of Senior Scientist and the leader of antenna group under the RF and Optical Department. His main research include antenna design and characterization for wireless applications. In particular, his current R&D focuses on small and broadband antennas/arrays for wireless systems, such as ultrawideband (UWB) systems, radio frequency identification (RFID) systems and medical imaging systems, microwave, mmW, submmW, and THz imaging systems. He has authored and coauthored over 110 technical papers published in international journals or presented at international conferences, and five book chapters. He holds 10 granted and filed patents.

Dr. Qing received six awards of advancement of science and technology in China. He is also the recipient of the IES Prestigious Engineering Achievement Award 2006, Singapore, and the ISAP 2010 Best Paper Award. He has

been a member of the IEEE Antennas and Propagation Society since 1990. He is serving as the Editor Board Member for the *International Journal of Microwave Science and Technology*. He also served the Guest Editor of the special issue “Antennas for Emerging Radio Frequency Identification (RFID) Applications” at *International Journal on Wireless & Optical Communications*. He has served as the TPC member and session chair for a number of conferences, was the organizer and chair for special sessions on RFID antennas at IEEE Antenna and Propagation Symposium 2007 and 2008, and was a member of the RFID Technical Committee (TC-24) of the IEEE MTT since 2009. He served as a reviewer for many prestigious journals such as the IEEE TRANSACTIONS ON ANTENNAS AND PROPAGATION, the IEEE TRANSACTIONS ON MICROWAVE THEORY AND TECHNIQUES, the IEEE ANTENNAS AND WIRELESS PROPAGATION LETTERS, the IEEE MICROWAVE AND WIRELESS COMPONENTS LETTERS, *IET Microwaves, Antennas, and Propagation*, and *IET-MAP, Electronic Letters*.



Zhijun Zhang (M'00–SM'04) received the B.S. and M.S. degrees from the University of Electronic Science and Technology of China, Chengdu, in 1992 and 1995, respectively, and the Ph.D. degree from Tsinghua University, Beijing, China, in 1999.

In 1999, he was a Postdoctoral Fellow with the Department of Electrical Engineering, University of Utah, where he was appointed a Research Assistant Professor in 2001. In May 2002, he was an Assistant Researcher with the University of Hawaii at Manoa, Honolulu. In November 2002, he joined Amphenol T&M Antennas, Vernon Hills, IL, as a Senior Staff Antenna Development Engineer and was then promoted to the position of Antenna Engineer Manager. In 2004, he joined Nokia Inc., San Diego, CA, as a Senior Antenna Design Engineer. In 2006, he joined Apple Inc., Cupertino, CA, as a Senior Antenna Design Engineer and was then promoted to the position of Principal Antenna Engineer. Since August 2007, he has been with Tsinghua University, where he is a Professor in the Department of Electronic Engineering. He is the author of *Antenna Design for Mobile Devices* (Wiley, 2011).

Dr. Zhang serves as Associate Editor of the IEEE TRANSACTIONS ON ANTENNAS AND PROPAGATION and the IEEE ANTENNAS AND WIRELESS PROPAGATION LETTERS.



Junfeng Xu (M'10) was born in Nanjing, China, in 1981. He received the B.S., M.S., and Ph.D. degrees from Southeast University, Nanjing, China, in 2003, 2006 and 2009, respectively, all in the radio engineering.

Since 2010, he has been with the Institute for Infocomm Research, Agency of Science, Technology, and Research, Singapore. He is currently holding the position of Scientist I under the RF and Optical Department. His current research include planar antenna and array design for millimeter-wave applications,

especially the 60-GHz band, the 140-GHz band, and the 270-GHz band. These antennas and arrays are based on the substrate-integrated technology on LTCC and PCB.

Dr. Xu is the first Recipient of the Best Paper Award at the 15th International Symposium on Antennas and Propagation (ISAP 2010), Macau. He serves as a Reviewer of the IEEE TRANSACTIONS ON ANTENNAS AND PROPAGATION and the IEEE ANTENNAS AND WIRELESS PROPAGATION LETTERS.



Zhenghe Feng (M'05–SM'08–F'12) received the B.S. degree in radio and electronics from Tsinghua University, Beijing, China, in 1970.

Since 1970, he has been with Tsinghua University, as an Assistant, Lecturer, Associate Professor, and Full Professor. His main research areas include numerical techniques and computational electromagnetics, RF and microwave circuits and antenna, wireless communications, smart antenna, and spatial-temporal signal processing.